Sensitive photoelectric sensing for 5-HMF detection

Xin He[a], Caiyun Jiang[a,b]*, Jie Yang[a], Shuangchao Sheng[a], Yuping Wang[a,c]*

[a] School of Chemistry and Material Science, Jiangsu Provincial Key Laboratory of

Materials Cycling and Pollution Control, Nanjing Normal University, Nanjing 210023,

China

[b] Jiangsu Engineering Research and Development Center of Food Safety, Department

of Health, Jiangsu Vocational Institute of Commerce, Nanjing 211168, China

[c] Jiangsu Key laboratory of Chemical Pollution Control and Resources Reuse, Nanjing

University of Science and Technology, Nanjing 210094, China

* Corresponding author: jiangcaiyun29@126.com; wangyuping@njnu.edu.cn

2.1 Characterization of materials

The structure of the material was analyzed by X-ray diffraction (XRD) by Cu-Kα rays (λ = 1.5406 A) with a scanning range of 5° - 90° and a scanning speed of 5 °/min. The surface morphology and microstructure of $SiO_2@TiO_2$ and $h-TiO_2$ nanospheres were observed using high-resolution thermal field emission scanning electron microscopy (FESEM) and H-7650 transmission electron microscopy (TEM). The elemental composition and chemical valence states of materials were determined with X-ray photoelectron spectroscopy (XPS). Brunauer-Emmett-Teller (BET) surface area test gave N_2 adsorption-desorption isotherm and the corresponding pore size distribution.
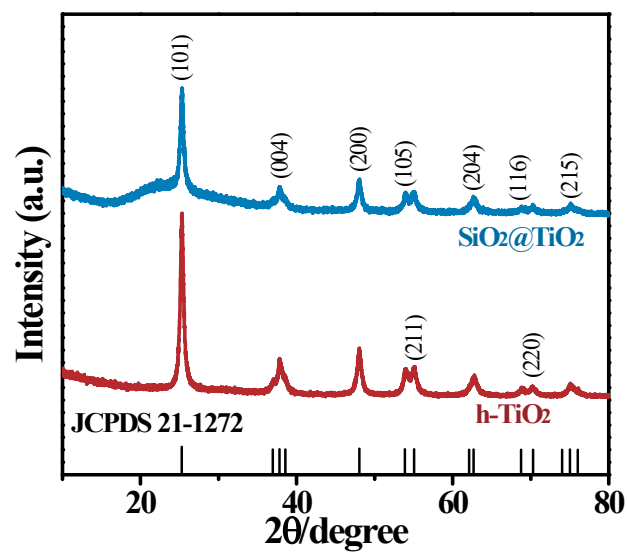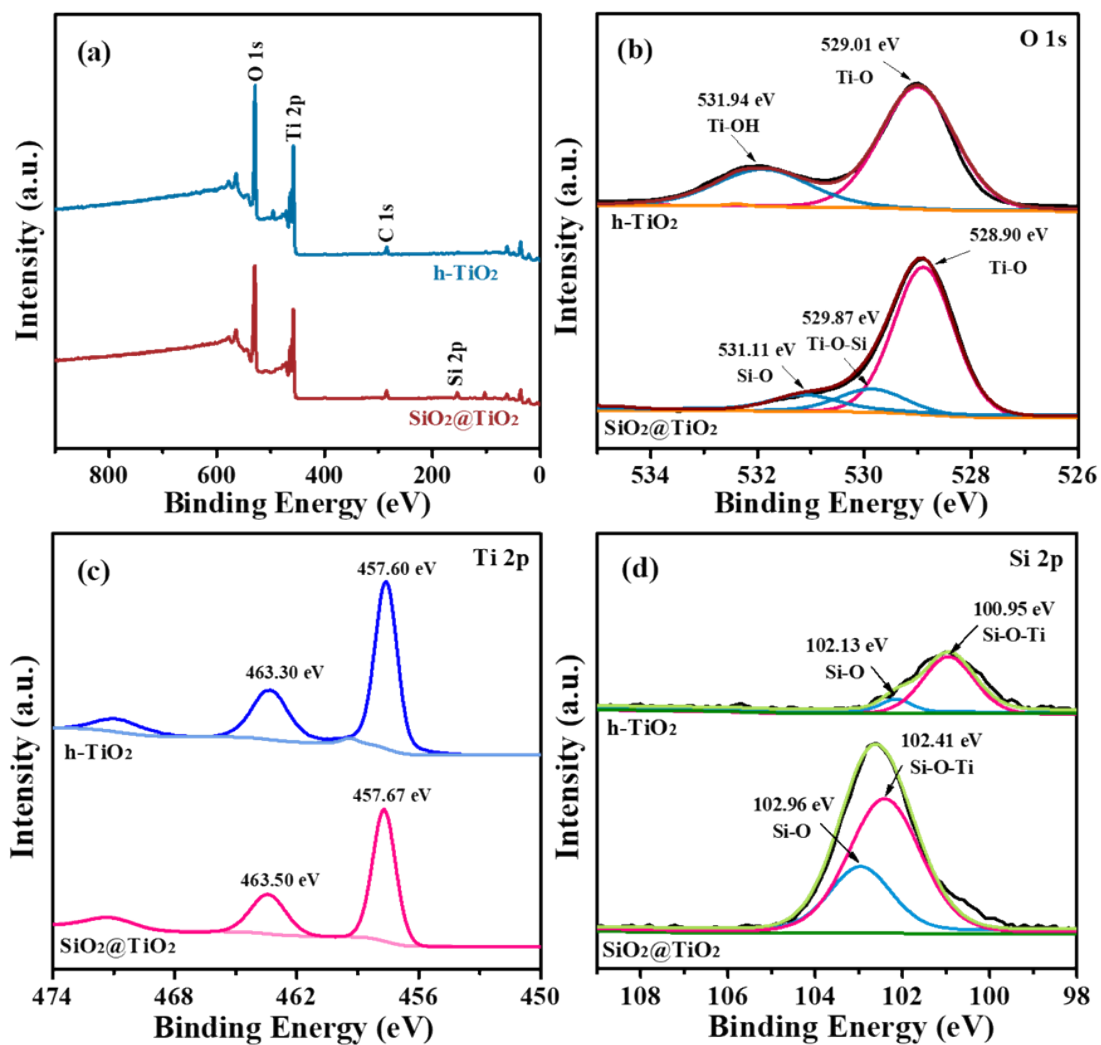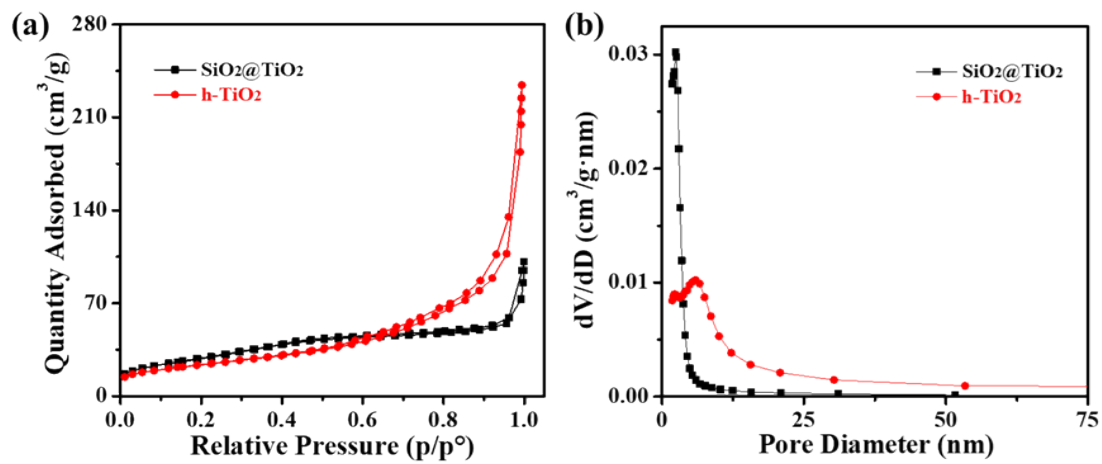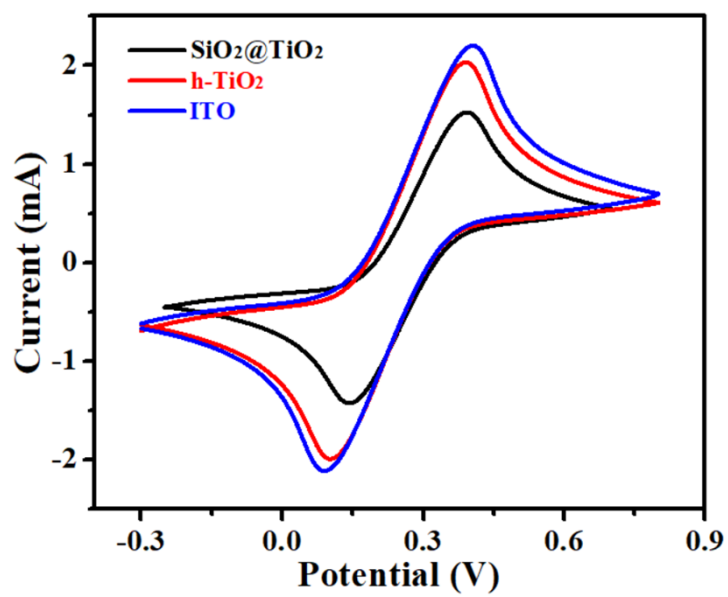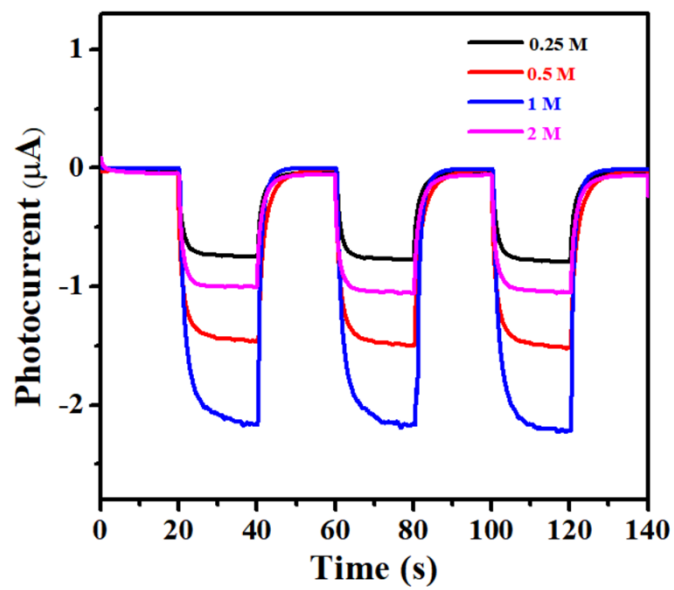
Fig. S1 XRD images of $SiO_2@TiO_2$ and h-TiO_2.

Fig. S2 (a) Full XPS spectra of SiO$_2$@TiO$_2$ and h-TiO$_2$; (b) O 1s, (c) Ti 2p, (d) Si 2p corresponding XPS spectra.
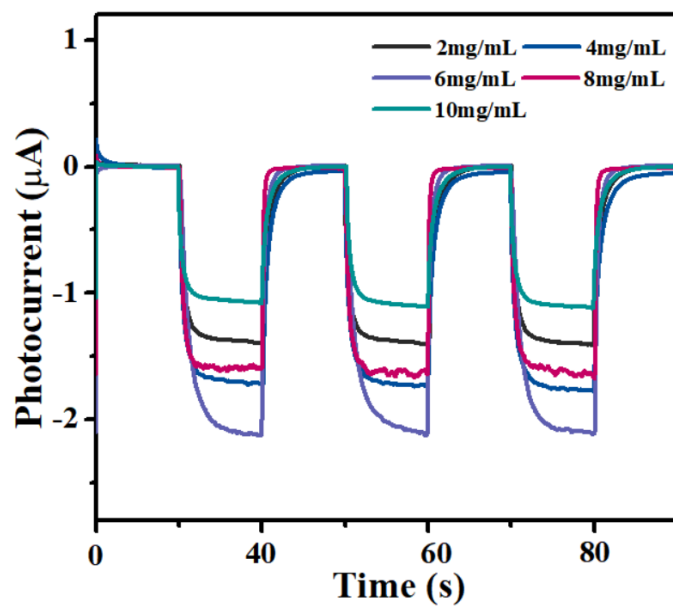
Fig. S3 (a) N_2 adsorption-desorption isotherms of $SiO_2@TiO_2$ and h-TiO_2; (b) BJH aperture profile.

Fig. S4 CV curves of $SiO_2@TiO_2$/ITO, h-TiO_2/ITO and blank ITO in $K_3[Fe(CN)_6]$ and $K_4[Fe(CN)_6]$ mixtures.
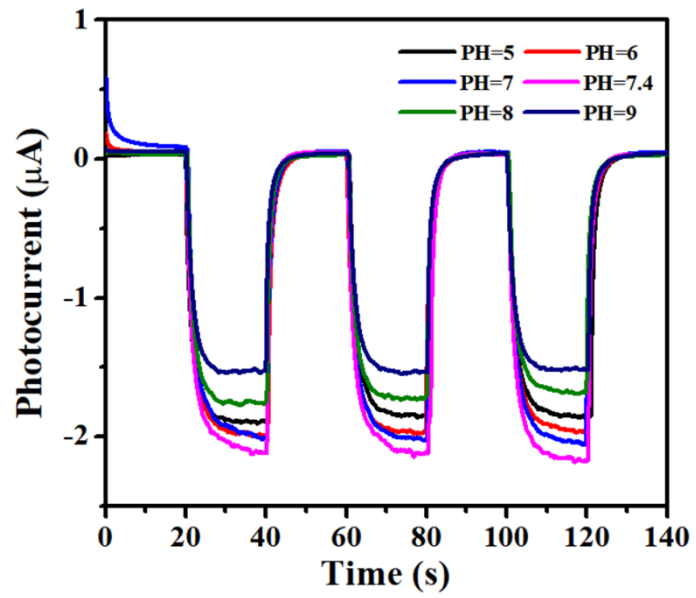
Fig. S5 h-TiO$_2$ photocurrent response obtained by etching SiO$_2$ with different concentrations of NaOH solution.

Fig. S6 Effect of concentration of photoactive material on photocurrent response.

Fig. S7 Effect of pH of electrolyte solution on photocurrent response of photoactive materials.

Table S1 Comparison of 5-HMF detection by different methods.

Analytical method	Linear range/μM	LOD/nM	References
PAD	0.200-396.5	237.89	S1
HPLC	216-2160	216002	S2
HPLC	6.20-92.5	18.5	S3
^{1}H NMR	95.2-537.5	95160	S4
ELISA	0-158.6	142.7	10
MEKC	7.90-198.2	3409.7	S5
MEKC	79.30-634.4	713.7	11
LC-MS	7.90-79.3	2616.9	S6
FAAS	31.70-1903.1	10071.1	S7
h-TiO$_2$ PEC	0.00001-0.100	0.001	this work

References

[S1]   H. Xu, A. C. Templeton and R. A. Reed, Quantification of 5-HMF and dextrose in commercial aqueous dextrose solutions, *J. Pharm. Biomed. Anal.*, 2003, **32**, 451–459.

[S2]   Y. H. Li and X. Y. Lu. Investigation on the origin of 5-HMF in Shengmaiyin decoction by RP-HPLC method, *J. Environ. Chem. Eng.*, 2005, **6**, 1015-21.

[S3]   N. Spano, L. Casula, A. Panzanelli, M. Pilo, P. Piu, R. Scanu, A. Tapparo and G. Sanna, An RP-HPLC determination of 5-hydroxymethylfurfural in honey: The case of strawberry tree honey, *Talanta*, 2006, **68,** 1390–1395.

[S4]   G. del Campo, I. Berregi, R. Caracena and J. Zuriarrain, Quantitative determination of caffeine, formic acid, trigonelline and 5-(hydroxymethyl) furfural in soluble coffees by 1H NMR spectrometry, *Talanta*, 2010, **81**, 367–371.

[S5]   Y. Foo Wong, A. Makahleh, K.M. Al Azzam, N. Yahaya, B. Saad and S. Amrah Sulaiman, Micellar electrokinetic chromatography method for the simultaneous determination of furanic compounds in honey and vegetable oils,

[S6]   D. Tomasini, M.R.F. Sampaio, S. S. Caldas, J. G. Buffon, F. A. Duarte and E. G. Primel, Simultaneous determination of pesticides and 5-hydroxymethylfurfural in honey by the modified QuEChERS method and liquid chromatography coupled to tandem mass spectrometry, *Talanta*, 2012, **99**, 380–386.

[S7]   R. Gürkan, A New Enrichment Method for Quantification of 5-Hydroxymethylfurfural by Indirect Flame Atomic Absorption Spectrometry in Honey and Jam Samples, *J AOAC Int.*, 2021, **104**, 682–692.